*This article appeared in the **International Journal of Heating, Ventilation, Air-Conditioning, and Refrigeration Research**, Volume 9, Number 2, April 2003, pp. 153-166.*

Use of Computational Fluid Dynamics for Calculating Flow Rates Through Perforated Tiles in Raised-Floor Data Centers

Kailash C. Karki, Amir Radmehr, and Suhas V. Patankar
Innovative Research, Inc.
3025 Harbor Lane N, Suite 300
Plymouth, MN 55447, USA

ABSTRACT

This paper describes a Computational Fluid Dynamics model for calculating airflow rates through perforated tiles in raised-floor data centers. The model is based on the assumption that the pressure in the space above the raised floor is uniform, which allows the calculation to be limited to the space below the raised floor. It uses a finite-volume method, the k-ε turbulence model, and a multigrid method. The model is applied to a real-life data center. The calculated results for velocity and pressure distributions are discussed. The flow rates through the perforated tiles are shown to be in good agreement with the measured values.

INTRODUCTION

Airflow Distribution in Data Centers

Data centers are used to house computer servers, telecommunications equipment, and data storage systems. The equipment, which dissipates a significant amount of heat, must be maintained at acceptable temperatures for reliable operation. The heat load can vary significantly across the computer room, and it changes with addition or reconfiguration of hardware. Therefore, to prevent equipment failure, just meeting the total cooling capacity or airflow requirement is not sufficient; special attention must be paid to the *distribution* of the cooling air.

Most data centers use the under-floor plenum below a raised floor to supply cold air to the equipment. The computer room air conditioner (CRAC) units push cold air into the plenum, from where it is introduced into the computer room via perforated floor tiles, cable cutouts, and floor grilles; see Fig. 1 for a typical floor layout. In these "raised-floor" data centers, the distribution of the air flow through the perforated tiles is governed by the size of the plenum, the arrangement and open area of the perforated tiles, the placement and flow rates of CRAC units, and the under-floor blockages like cables and pipes. The complex flow in the plenum sets up a pressure distribution, which controls the flow through the perforated tiles.

Due to the interactive effect of different parameters, the resulting flow distribution is usually not uniform. This means that the computer servers in some areas get too much air, while others get too little. Whenever the cooling-air requirements of any server are not met, its cooling is compromised. The necessary and sufficient condition for good thermal management is supplying the required airflow through the perforated tile(s) located at the inlet of each computer server.

Available Design Procedures

Currently the data center floor layouts are designed using empirical guidelines based on limited measurements. These guidelines do not consider the complex fluid dynamics processes that control the flow rate distribution. Consequently, the layouts do not produce the expected flow rates and must be modified. However, because modifications in one region of the floor influence flow rates throughout the floor, considerable trial and error is involved in identifying adjustments that will yield the desired changes in the flow rate distribution. This design practice is time consuming and expensive, and often the resulting arrangement is not optimum. Computational Fluid Dynamics (CFD) modeling offers a more scientific and comprehensive design approach.

Computational simulation can be used for a quick setup of any proposed layout, any desired placement of CRAC units and perforated tiles, and any imagined failure scenario. The "computational" trial-and-error process is preferable for two reasons. First, performing a

simulation is much faster and more economical than building an actual layout. Second, the computed results provide not only the flow rate distribution but also the underlying velocity and pressure fields and thus explain the physics behind the flow rate variation. This understanding is useful in guiding the computational trial-and-error process in the optimum direction.

Outline of an Efficient CFD Model

The calculation of flow rates through perforated tiles requires information on the pressure distributions in the plenum and in the computer room above the raised floor. Pressure variations within the computer room are generally small compared to the pressure drop across the perforated tiles. (This observation will be discussed in detail later.) Thus, relative to the plenum, the pressure just above the perforated tiles can be assumed to be uniform. With this simplification, the flow rates can be calculated solely from the knowledge of the pressure field in the plenum, without consideration of the flow field in the computer room. The present study uses a CFD model to calculate the three-dimensional (3D) velocity and pressure distributions in the plenum. The local pressure drop across individual perforated tiles then determines the corresponding flow rate.

We note that the flow rates can also be obtained from a CFD model of the entire space above and below the raised floor. But such a model is overly complex if only the flow rates are of interest.

Related Prior Work

There is very limited prior work on the prediction of the flow rates through perforated tiles. Kang et al. (2000) have presented a computational model in which the plenum is assumed to be at a *uniform* pressure. This assumption eliminates the need for calculating velocity and pressure distributions in the plenum. However, such a model is inappropriate if the horizontal air velocities in the plenum are significant and introduce appreciable pressure variations. These situations necessitate the use of a CFD model to calculate the pressure distribution in the plenum.

In a previous investigation (Schmidt et al., 2001), we had described a CFD model based on the depth-averaged (two-dimensional) representation of velocity and pressure distributions in the plenum and presented its validation using measurements in a prototype data center with plenum height of 8.5 inches (0.216 m). The model neglects variations along the height of the plenum; it is, therefore, appropriate for plenums with small heights. This depth-averaged model correctly predicts the nonuniformity in the flow rate distribution and the occurrence of reverse flow (flow into the plenum) near the CRAC units.

With the exception of the two studies cited above, the focus of CFD modeling in data centers has been on fluid flow and heat transfer in computer rooms. (There are no published reports on CFD modeling of a complete raised-floor data center.) A selected number of publications on airflow

modeling in computer rooms and similar enclosures are reviewed here. Awbi and Gan (1994) have reported airflow and temperature distributions within offices. Kiff (1995) has reported results for rooms populated with telecommunications equipment. Schmidt (1997) has analyzed an office size data-processing room and has compared the predicted temperature and velocity fields with measurements. Patel et al. (2001) have presented predictions for flow and temperature distributions in a prototype data center cooled by a set of modular heat exchanges in the ceiling and have compared their results with measurements.

Outline of the Paper

The aim of this paper is to predict flow rates through perforated tiles using a three-dimensional (3D) CFD model applied only to the space *under* the raised floor. The computational model uses a finite-volume method, the k-ε turbulence model, and a multigrid method. The present model is implemented in a software package (Innovative Research, Inc., 2001). The 3D model, unlike the depth-averaged model described in Schmidt et al. (2001), can be applied to any plenum height. For small heights (less than 12 inches [0.30 m]), the results from the two models are identical. The 3D model has been used to predict flow rate distribution in an actual data center, and the results are compared with measurements.

Focus of the Paper

Although the paper ends with an application of the proposed method to a specific data center, the particular results are not the focus of the paper. They are included as an illustration and are used to validate the method by comparison with measurements. They help to describe the type of velocity and pressure variation that are normally found in the under-floor space.

The main contribution of the paper lies in the identification of three important concepts:

(a) Delivering the right amount of airflow at the inlet of each computer server holds the key to the management of cooling in a data center.

(b) A CFD model can offer a flexible, scientific, and comprehensive approach to the prediction of the airflow rates.

(c) It is sufficient to limit the model to the space below the raised floor and thus achieve substantial economy of computational effort.

THE COMPUTATIONAL MODEL

Governing Equations

The mathematical model for flow in the plenum is formulated from the incompressible form of the Navier-Stokes equations, together with the k-ε turbulence model (Launder and Spalding, 1974). The flow is assumed to be steady and isothermal. The mass and momentum equations can be expressed in Cartesian tensor notation as:

$$\frac{\partial}{\partial x_i}(\rho u_i) = 0 \tag{1}$$

$$\frac{\partial}{\partial x_i}(\rho u_i u_j) = \frac{\partial}{\partial x_i}\left(\mu_t \frac{\partial u_j}{\partial x_i}\right) - \frac{\partial p}{\partial x_j} + S_j \tag{2}$$

Here ρ is density, u_j is the velocity component in the j^{th} coordinate direction, μ_t is the turbulent viscosity, p is pressure, and S_j denotes source terms for the velocity component u_j. In the k-ε model, the turbulent viscosity is given by

$$\mu_t = c_\mu \rho \frac{k^2}{\varepsilon} \tag{3}$$

where c_μ is a constant, k is the turbulence kinetic energy, and ε is its rate of dissipation. The parameters k and ε are obtained by solving two additional differential equations; for complete details, see Launder and Spalding (1974).

Boundary Conditions

Walls. At the walls of the plenum and at other solid surfaces, the usual no-slip boundary conditions are used. For wall shear stress and turbulence quantities, the standard wall-function treatment described in Launder and Spalding (1974) is employed.

Inflow through CRAC units. The flow exiting the CRAC unit outlets is treated as inflow into the plenum. All dependent variables are assumed known at the inflow. The inlet vertical velocity is deduced from the CRAC flow rate and the outlet open area. The horizontal velocity components are assumed to be zero.

Flow through perforated tiles. The flow rate through a perforated tile is calculated using the relationship

$$\Delta p = R|Q|Q \tag{4}$$

where Δp is the pressure drop across the tile, Q is the volumetric flow rate, and R is the flow resistance factor. The pressure drop Δp is the difference between the plenum pressure just below a tile and the ambient pressure above the raised floor. As discussed below, the ambient pressure is considered to be uniform. The flow resistance factor R is related to the loss coefficient (K) for the tile as

$$R = \frac{1}{2}\frac{\rho}{A^2}K \tag{5}$$

where ρ is air density and A is the total tile area.

For a perforated tile, the flow breaks up into a number of small high-velocity jets, which coalesce into a small-velocity stream. The pressure loss is primarily due to the loss of kinetic energy of the high-velocity jets. An empirical formula for K, supported by a large number of measurements, is (Idelchik, 1994)

$$K = \frac{1}{f^2}\left(1 + 0.5(1-f)^{0.75} + 1.414(1-f)^{0.375}\right) \tag{6}$$

where f is the fractional open area of the tile. The pressure drop given by this formula agrees well with the data available from the manufacturers of perforated tiles. The formula gives a K of 42.8 for a perforated tile with 25% open area.

The direction of flow through a perforated tile depends on the sign of Δp. If the local pressure under a tile falls below the ambient pressure ($\Delta p < 0$), flow through the tile will be directed towards the plenum, that is, there will be reverse flow.

Uniformity of Pressure Above the Perforated Tiles

An important aspect of the computational model presented here is the ability to limit the calculation to the space *below* the raised floor, without the need for performing the computation in the very large computational domain *above* the raised floor. This substantial reduction in the size of the computational space is achieved by assuming that the pressure just above the perforated tiles is uniform. Since the validity of the proposed approach rests on this assumption, its basis is discussed below.

In general, the pressure in the plenum is higher than the pressure above the raised floor. It is this pressure difference that overcomes the flow resistance on the perforated tiles. The dimensionless pressure drop K (the loss coefficient) for the standard perforated tiles with 25% open area is around 43. This means that the pressure drop is equal to 43 velocity heads. When the air streams emerging from the perforated tiles mix or dissipate, pressure changes of the order of *one* velocity head are produced. Since this number is small compared to 43, the pressure just above the raised floor can be considered uniform.

In the computer room, the only other region of possible pressure variations is where the air returns to the CRAC units. The return air travels along the ceiling and is drawn into the large opening at the top of the CRAC unit. Near the opening, the velocities can be large, causing significant pressure variation. However, the CRAC units are usually 6 ft (1.8 m) tall. Therefore, this region is sufficiently away from the raised floor and does not influence the pressure distribution just above the perforated tiles.

The above arguments are sufficient to justify the assumption of uniform pressure. The comparison with measurements, reported later in the paper, provides additional validation of this assumption.

NUMERICAL SOLUTION PROCEDURE

Derivation of Discrete Equations

The governing equations are discretized on a Cartesian grid using the finite-volume method described by Patankar (1980). A staggered grid arrangement is used in which pressure and other scalar quantities (e.g., the turbulence kinetic energy and rate of dissipation) are located at the center of a control volume and the velocity components are located at the control-volume faces. The convection and diffusion fluxes are approximated using the power-law differencing scheme.

Solution of Discrete Equations

Separate procedures are used to solve the equations for the fluid flow variables and the equations for turbulence parameters. The continuity and momentum equations are solved in a coupled manner using the additive correction multigrid method (described below). The k and ε equations are solved only on the finest grid, sequentially using the Stone's algorithm (Stone, 1968). These equations are strongly coupled through their source terms. This coupling is resolved by repeating the solution of the k and ε equations until a prescribed convergence criterion is satisfied. During this cycle for the k-ε subset, the discretization coefficients are kept fixed but the source terms are updated using the latest values of k and ε.

Additive Correction Multigrid (ACM) Method

Iterative solvers, like the Gauss-Seidel method, are efficient in reducing the high frequency components of error (those with wavelengths comparable to the grid spacing), but are ineffective in removing the low frequency components. Multigrid methods (e.g., Brandt, 1977; Briggs, 1987) recognize that low frequencies on a given grid appear as high frequencies on a coarser grid and can thus be smoothed by applying the solver on a coarser grid. These methods solve the problem on a series of successively coarser grids so that all frequency components are reduced at comparable rates.

The ACM method (Sathyamurthy and Patankar, 1994; Hutchinson et al., 1988) obtains the equations on a coarse grid directly from the fine-grid equations by applying the block-correction strategy of Settari and Aziz (1973). Therefore, discretization is required on the finest grid only. (This is in contrast to other multigrid methods, where the equations are discretized on all grids.) The coarse grid equation for a particular block of fine grid nodes is constructed by combining the corresponding fine-grid equations so that conservation is maintained over the coarse grid block. The corrections calculated on the coarse grid are assumed uniform over each block of fine grid nodes.

The continuity and momentum equations are solved in a coupled manner. These equations along a vertical line are combined to obtain an equation for pressure corrections, which is solved using the TriDiagonal Matrix Algorithm (e.g. Patankar, 1980). The resulting pressure corrections are then used to update the velocity components and pressures.

The important steps in the present implementation of the multigrid method are outlined here for two grid levels; the generalization to multiple grid levels is straightforward.

1. Calculate the discretization coefficients on the fine grid.

2. Perform specified number of relaxation sweeps on the fine grid.

3. Solve the correction equations on the coarse grid.

4. Add the corrections to the fine-grid solution and perform specified number of sweeps.

5. Return to Step 1 and repeat until convergence is achieved.

Formation of Coarse Grids

The coarse grid blocks are formed by following the standard practice of combining $2 \times 2 \times 2$ set of fine-grid control volumes, except for the near-boundary blocks, which contain a different number of control volumes if the fine grid has an odd number of control volumes in a particular direction. For the calculation domain considered here, the vertical dimension is much smaller

than the two horizontal dimensions and contains much fewer control volumes. Such a grid arrangement does not allow coarsening in the vertical direction beyond a few grid levels, that is, once the number of blocks in the vertical direction reaches the specified lower limit, usually 1. The subsequent coarser grids are formed by combining the control volumes in the horizontal directions only, until the entire domain is spanned by a very coarse grid.

APPLICATION OF THE MODEL

Details of Data Center

The data center floor dimensions are 130 ft × 73 ft (39.6 m × 22.3 m). It has 11 CRAC units, each with airflow rate of 12,400 CFM (5.85 m^3/s), and over 200 perforated tiles (side dimension of 2 ft [0.61 m]) with 25% open area. The plenum height is 30 inches (0.76 m). The CRAC units are arranged in a "distributed" manner, instead of being located along the walls of the room. This arrangement ensures that each perforated tile has a CRAC unit in its proximity, thus allowing better control over the flow rate distribution. The CRAC units have two blowers, each with a rectangular outlet opening; the footprint is shown in Fig. 2.

In addition to the computer equipment to which cold air is supplied through the perforated tiles, the data center has provision for racks that draw cold air directly from the plenum, through cutouts on the floor panels. There are additional cable openings on numerous floor panels. (In the subsequent discussion, the term perforated tile will be used in a generalized sense to include the panels with cutouts and cable openings.) The plenum contains blockages like cables and pipes. There are regions, especially near the CRAC units, where these blockages occupy a significant portion of the plenum height. The room also has a number of support columns. Figure 3 shows the arrangement of CRAC units and perforated tiles on the floor. Here colors indicate different types of perforated tiles. Figure 4 gives an indication of the under-floor blockages.

Flow Measurement Tool

A flow measuring hood was used to measure the volumetric airflow rates through the perforated tiles. This tool, shown in Fig. 5, measures flow rates by reading average velocity as air moves through a cross section with known dimensions. The air to be measured is captured by the hood assembly and then directed past a square manifold that senses flow at 16 points. The manifold is connected to a velocity measurement tool that uses a mechanical swinging vane technology. The system can sense airflow in both directions. The flow measuring hood provides three ranges: 0 to 200 CFM (0 to 0.0944 m^3/s), 100 to 600 CFM (0.0472 m^3/s to 0.283 m^3/s), and 400 to 1400 CFM (0.189 m^3/s to 0.66 m^3/s). The accuracy is ±5% of the full scale. In the lowest range, the tool uses an adapter screen to reduce the effective area through which the air flows, causing an increase in velocity past the manifold.

Computational Details

The computer model incorporates complete details of the floor, the support structures and under-floor pipes and cables that represent significant blockage, the perforated tiles, and the geometry of the CRAC unit outlets.

The flow resistance factors for perforated tiles are calculated using Eqs. (5) and (6), presented earlier.

The calculation domain is represented in a Cartesian coordinate system. Geometries that do not fit neatly into this coordinate system are represented by a series of rectangular steps. These geometries include under-floor blockages of non-rectangular shapes. The standard "wall" boundary conditions are applied at the internal fluid-solid interfaces.

Calculations were made on a nonuniform grid comprising 141 × 97 × 10 (x, y, z) control volumes. The grid lines were densely packed near the CRAC unit outlets, the raised floor, and the sub floor. In the horizontal plane, the grid spacing was 6 inch in the regions containing the CRAC outlet openings and 12 inch elsewhere. This final grid was arrived at by performing grid sensitivity studies on smaller data centers, which indicated that halving the grid spacing resulted in less than 5% difference in the flow rates through the perforated tiles. This level of accuracy is considered adequate, considering the uncertainties in problem definition, such as the exact flow rate through the CRAC units, the precise details of the blockages, etc., that are likely to be encountered in practice. For this grid, the execution time was about 30 minutes on a personal computer with 1.5 GHz processor speed and 512 MB RAM.

Results and Discussion

Details of the Flow Field

The results are presented via streaklines (streamtraces) and pressure contours on selected planes. The streaklines are calculated using the in-plane velocity components for the planes. To enable better visualization of streakline plots, the vertical (z) dimension has been enlarged by a factor of 5 in Fig. 6 and by a factor of 10 in Fig. 7.

Figure 6 shows the results on two transverse (x = constant) planes, one passing through the CRAC units and other between two rows of CRAC units. The flow field on a particular plane depends on its position with reference to the CRAC units and the arrangement of perforated tiles. Figure 6(a) shows the flow pattern and pressure distribution through the transverse plane x = 33 ft; this plane passes through a vertical row of CRAC units and contains three units. From each CRAC unit, air enters the plenum in the form of two jets (six jets for three CRAC units), one for each outlet opening (see Fig. 2 for details). The pressure is low at the inflow points (CRAC unit outlets), increases along the length of the jet, and attains the maximum value in the impingement

zone. Under each CRAC unit, the two peaks in the pressure distribution correspond to the two inlet jets. The jets impinge on the sub floor, spread horizontally, and turn 90 deg. There is flow entrainment near the jets. Pressure variation is noticeable only in the vicinity of the CRAC units; elsewhere pressure is nearly uniform.

Figure 6(b) shows the results on the plane x = 49 ft, roughly midway between two rows of CRAC units. Near the raised floor, pockets of low pressure develop at the perforated tile locations. The air movement in the perforated tile region is in the upward direction. In the region with no tiles, the flow is horizontal.

The results on the vertical (y = const) planes also follow the general trends discussed above. Figure 7 shows the results on the plane y = 11 ft, which passes through the row of CRAC units near the south (y = 0) wall. The air movement is primarily in the vertical direction, to supply air to the perforated tiles. On this plane, there is very little interaction between adjacent jets, because of the large spacing between the CRAC units.

Results presented in Figs. 6 and 7 show that gradients in the vertical (z) are confined primarily to the regions close to the CRAC units. Away from the CRAC units, horizontal velocities and pressures are nearly uniform, especially in regions where there are no perforated tiles.

Next, results on two horizontal planes are presented. Figure 8(a) shows the pressure distribution and projected velocity vectors on a horizontal plane near the sub floor. The pressure is higher at the locations where the inlet jets impinge. After impingement, the flow spreads horizontally. The flow pattern near the impingement zone, however, varies with the location of the CRAC unit. For units close to walls, the horizontal flow is primarily in the forward direction; for other units, the flow spreads in all directions.

Figure 8(b) shows the pressure distribution and streaklines on a horizontal plane just below the raised floor. Pressure is lower under the perforated tiles; the pockets of low pressure mimic the perforated tile pattern. The horizontal flow is mostly directed along the positive x axis.

The streaklines for the entire calculation domain are shown in Fig. 9. This figure gives an indication of the three-dimensional nature of the flow in the plenum.

Flow Rates Through Perforated Tiles

The predicted flow rate distribution is shown in Figure 10. The flow rates range from 100 to 500 CFM (4.72×10^{-2} to 0.236 m^3/s). The lower flow rates are for the panels with cable openings and cutouts, where the open area is between 5 and 15 %. The flow rates are lower near the CRAC units, where the horizontal velocities are large and pressures are low, and increase away from the CRAC units, as the horizontal velocities decrease and the pressures increase. Further, the nonuniformity in flow rates is more pronounced near the CRAC units, where horizontal pressure

variations are large. The flow rates are nearly uniform, and largest, for the perforated tiles placed midway between the rows of CRAC units.

Comparison with Measurements

The predicted and measured flow rates for 25% open tiles along selected columns, marked A through F in Fig. 10, are shown in Fig. 11. In general, the flow rates are in good agreement. The model correctly captures the observed nonuniformities in the flow rate distribution. For columns A, B, and C, the regions of lower flow rates—near tiles 2 and 3, 5 and 6, and 14 and 15—correspond to the low-pressure regions in the vicinity of the three CRAC units near these columns. These low-pressure regions are created due to the expansion of the jets and are responsible for the entrainment of surrounding fluid into the jets. Similarly, the regions of low flow rates in columns E and F lie close to the two CRAC units near these columns. Column D is away from the CRAC units, and the pressure under these tiles is nearly uniform, leading to a uniform flow rate distribution.

The comparison shows a few discrepancies between predictions and measurements. When a complex practical situation is simulated by a theoretical model, such departures are inevitable and their exact cause is difficult to ascertain. Since the discrepancies are small for practical purposes, the model is recommended for routine use in management of airflow in data centers.

CONCLUDING REMARKS

We have presented a Computational Fluids Dynamics model for calculating airflow distribution through perforated tiles in raised-floor data centers. A key ingredient of the computational model is the assumption that, relative to the plenum, the pressure above the tiles is uniform. This assumption allows the calculation to be limited just to the space below the raised floor, leading to substantial economy of computational effort compared to a model that covers the entire data center.

To illustrate the use of the model and to validate the results, it is applied to an actual data center, for which airflow rates are measured. The predicted flow rates through the perforated tiles are in good agreement with the measured values. The model gives an insight into the physical processes that control the distribution of airflow through the perforated tiles.

ACKNOWLEDGMENTS

We thank Engineering Design Group, Inc., Washington, D.C., for giving us access to the particular data center. Shadi Makarechi, Amir Raoufi, and John Garner provided guidance in preparing the measurement plan and in making the measurements.

REFERENCES

Awbi, H.B. and G. Gan, 1994, Prediction of Airflow and Thermal Comfort in Offices, *ASHRAE Journal*, Vol. 36, No. 2, pp. 17 – 21.

Brandt, A., 1977, Multilevel Adaptive Solutions to Boundary Value Problems, Mathematics of Computations, Vo. 31, pp. 333 – 390.

Briggs, W., 1987, *A Multigrid Tutorial*, Society of Industrial and Applied Mathematics.

Hutchinson, B.R., P.F. Galpin, and G.D. Raithby, 1988, Application of Additive Correction Multigrid Method to the Coupled Fluid Flow Equations, *Numerical Heat Transfer*, Vol. 13, pp. 133 – 147.

Idelchik, I.E., 1994, *Handbook of Hydraulic Resistance*, CRC Press, Florida.

Innovative Research, Inc., 2001, TileFlow: A Simulation Tool for Airflow Distribution in Raised-Floor data Centers.

Kang, S., R. Schmidt, K. Kelkar, A. Radmehr, and S. Patankar, 2000, A Methodology for the Design of Perforated Tiles in Raised Floor Data Centers Using Computational Flow Analysis. ITHERM 2000 Las Vegas, N. V., Proceedings Vol. 1, pp. 215 – 224.

Kiff, P., 1995, A Fresh Approach to Cooling Network Equipment, *British Telecommunications Engineering*.

Launder, B.E. and D.B. Spalding, 1974, The Numerical Computation of Turbulent Flows, *Computer Methods in Applied Mechanics and Engineering*, Vol. 3, pp. 269 – 289.

Patankar, S.V., 1980, *Numerical Heat Transfer and Fluid Flow*, Taylor and Francis.

Patel, C.D., C.E. Bash, C. Belady, L. Stahl, and D. Sullivan, 2001, Computational Fluids Dynamics Modeling of High Compute Density Data Centers to Assure System Air Inlet Specifications, Paper No. IPACK2001-15622, Proceedings of InterPack'01, The Pacific Rim/ASME International Electronic Packaging Technical Conference and Exhibition, July 8-13, 2001, Kauai, Hawaii, USA.

Sathyamurthy, P.S. and S.V. Patankar, 1994, Block-Correction-Based Multigrid Method for Fluid Flow Problems, *Numerical Heat Transfer, Part B (Fundamentals),* Vol. 25, pp. 375 – 394.

Schmidt, R.R., 1997, Thermal Management of Office Data Processing Centers, Interpack'97, Hawaii.

Schmidt, R.R., K.C. Karki, K.M. Kelkar, A. Radmehr, and S.V. Patankar, 2001, Measurements and Predictions of the Flow Distribution Through Perforated Tiles in Raised-Floor Data Centers, Paper No. IPACK2001-15728, Proceedings of InterPack'01, The Pacific Rim/ASME International Electronic Packaging Technical Conference and Exhibition, July 8-13, 2001, Kauai, Hawaii, USA.

Settari, A. and K. Aziz, 1973, A Generalization of Additive Correction Methods for the Iterative Solution of Matrix Equations*, SIAM Journal of Numerical Analysis*, Vol. 10, pp. 506 – 521.

Stone, H.L, 1968, Iterative Solution of Implicit Approximations of Multidimensional Partial Differential Equations, *SIAM Journal of Numerical Analysis*, Vol. 5, pp. 530 – 558.

List of Figure Captions

Figure 1. Schematic of a data center plenum, showing CRAC units, perforated tiles, and under-floor blockages.

Figure 2. Footprint of CRAC unit (dimensions in inch).

Figure 3. Floor layout showing perforated tiles and CRAC units.

Figure 4. Under-floor pipes and cables.

Figure 5. Flow measuring hood.

Figure 6. Pressure distribution and streaklines on two transverse planes.
(a) x = 33 ft, (b) x = 49 ft. (Pressure values in inch of water.)

Figure 7. Pressure distribution and streaklines on the vertical plane at y = 11 ft. (Pressure values in inch of water.)

Figure 8. Flow patterns and pressure distributions on horizontal planes.
(a) Near the sub floor, (b) Near the raised floor. (Pressure values in inch of water.)

Figure 9. Streaklines for the complete plenum.

Figure 10. Predicted flow rates through perforated tiles.

Figure 11. Comparison of measured and calculated flow rates for selected columns of tiles. The columns are identified in Fig. 10.

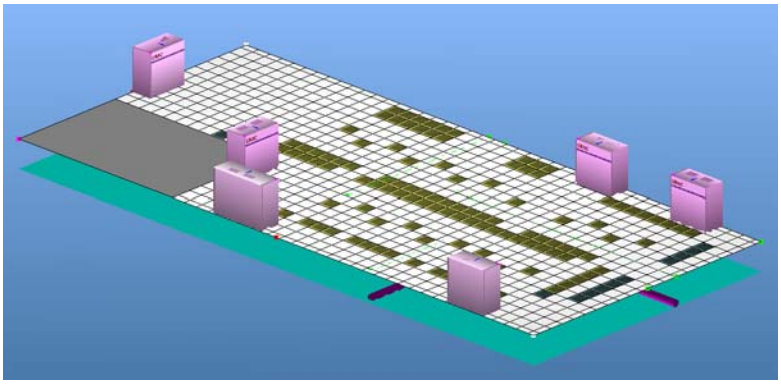

Figure 1
Schematic of a data center plenum, showing CRAC units, perforated tiles, and under-floor blockages.

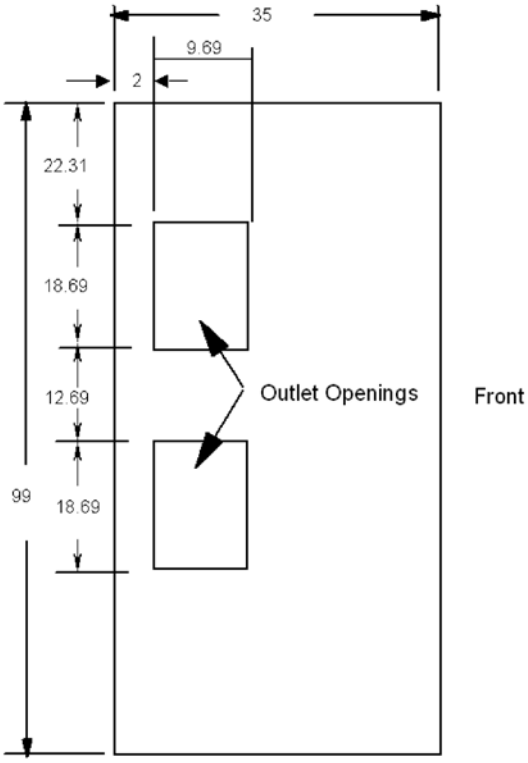

Figure 2
Footprint of CRAC unit.

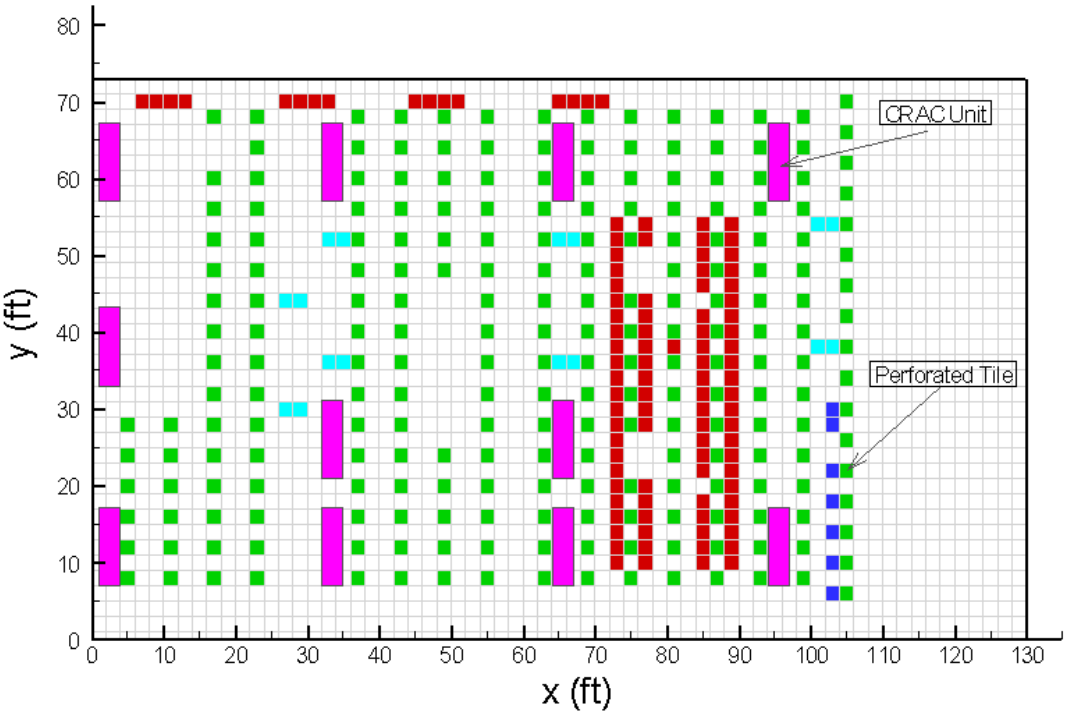

Figure 3
Floor layout showing perforated tiles and CRAC units.

Figure 4
Under-floor pipes and cables.

Figure 5
Flow measuring hood.

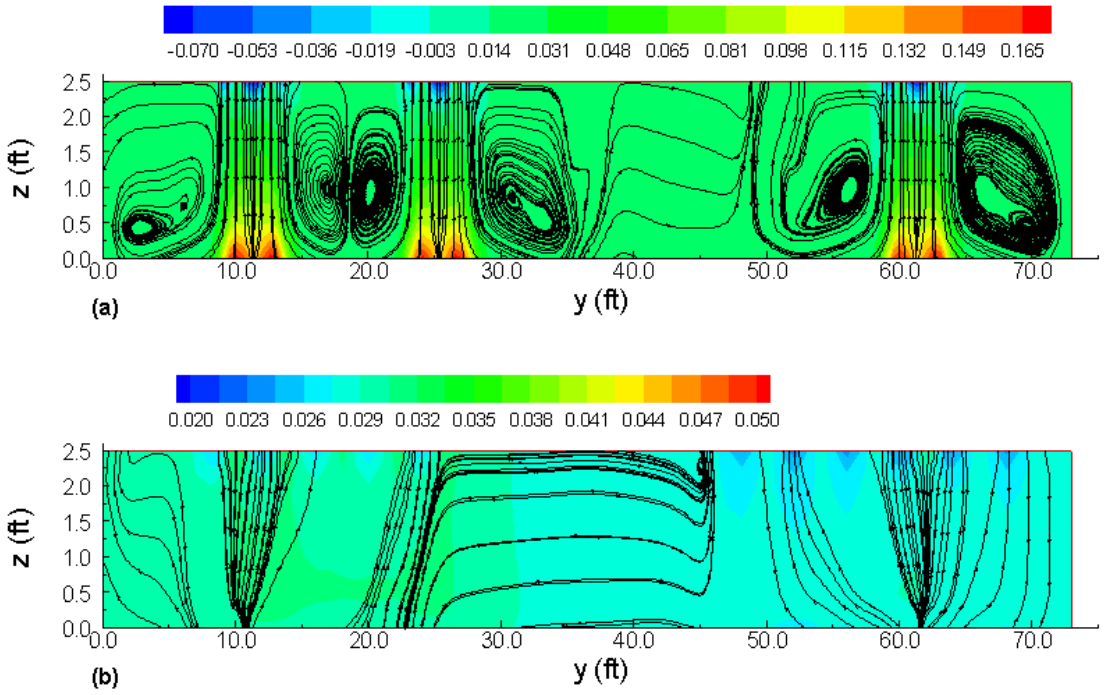

Figure 6
Pressure distribution and streaklines on two transverse planes.
(a) x = 33 ft, (b) x = 49 ft. (Pressure values in inch of water.)

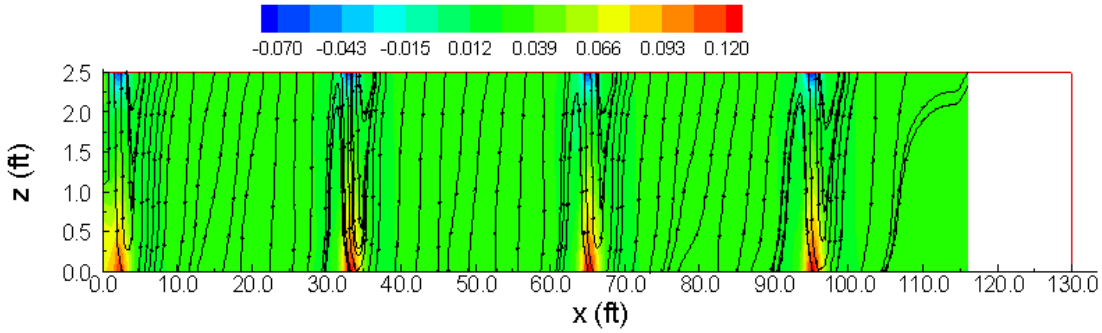

Figure 7
Pressure distribution (inch water) and streaklines on vertical plane at y = 11 ft. (Pressure values in inch of water.)

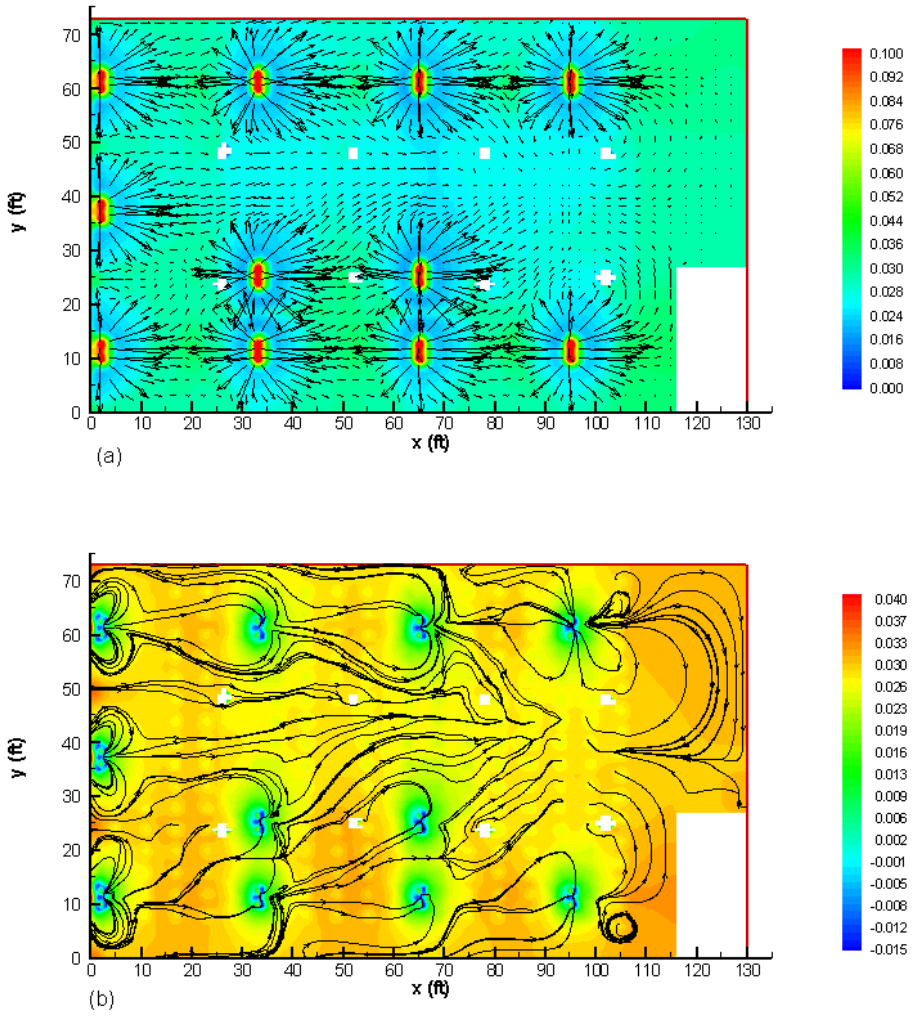

Figure 8
Flow patterns and pressure distributions on horizontal planes.
(a) Near the sub floor, (b) near the raised floor. (Pressure values in inch of water.)

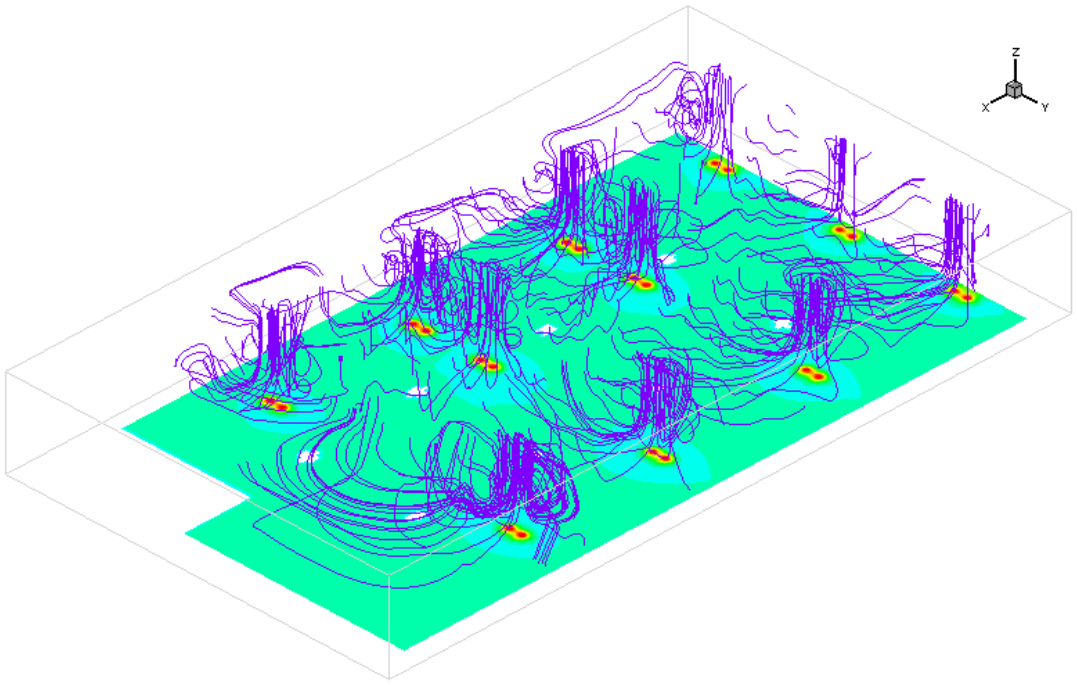

Figure 9
Streaklines for the full plenum.

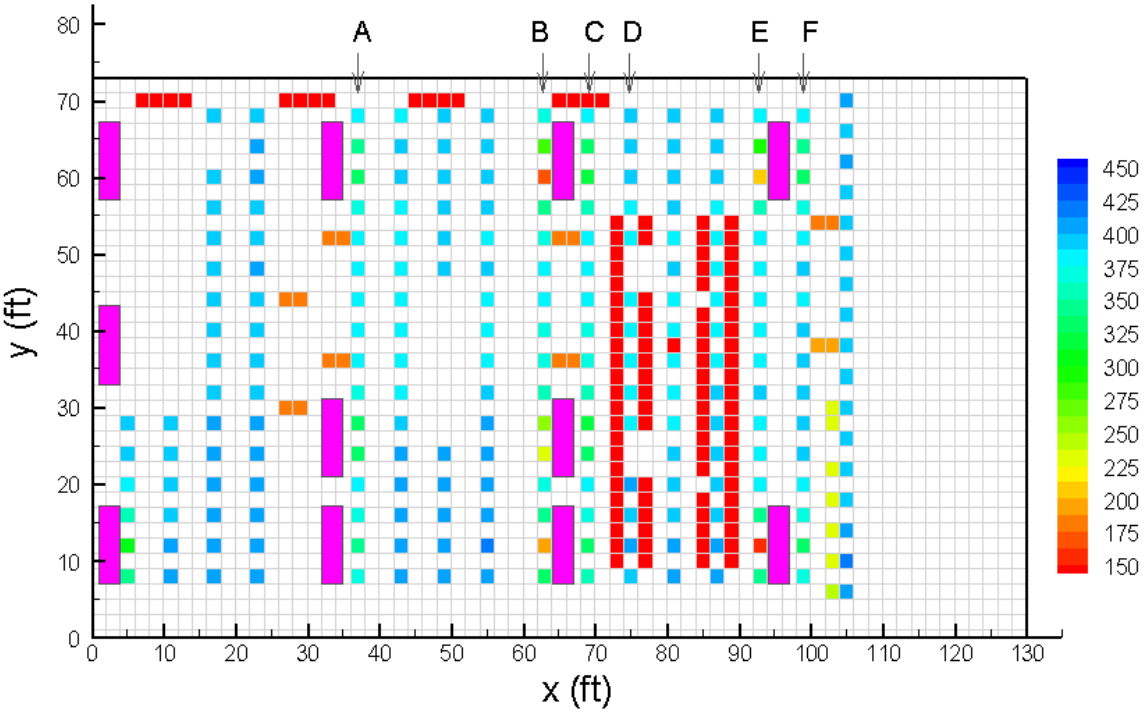

Figure 10
Predicted flow rates (CFM) through perforated tiles.

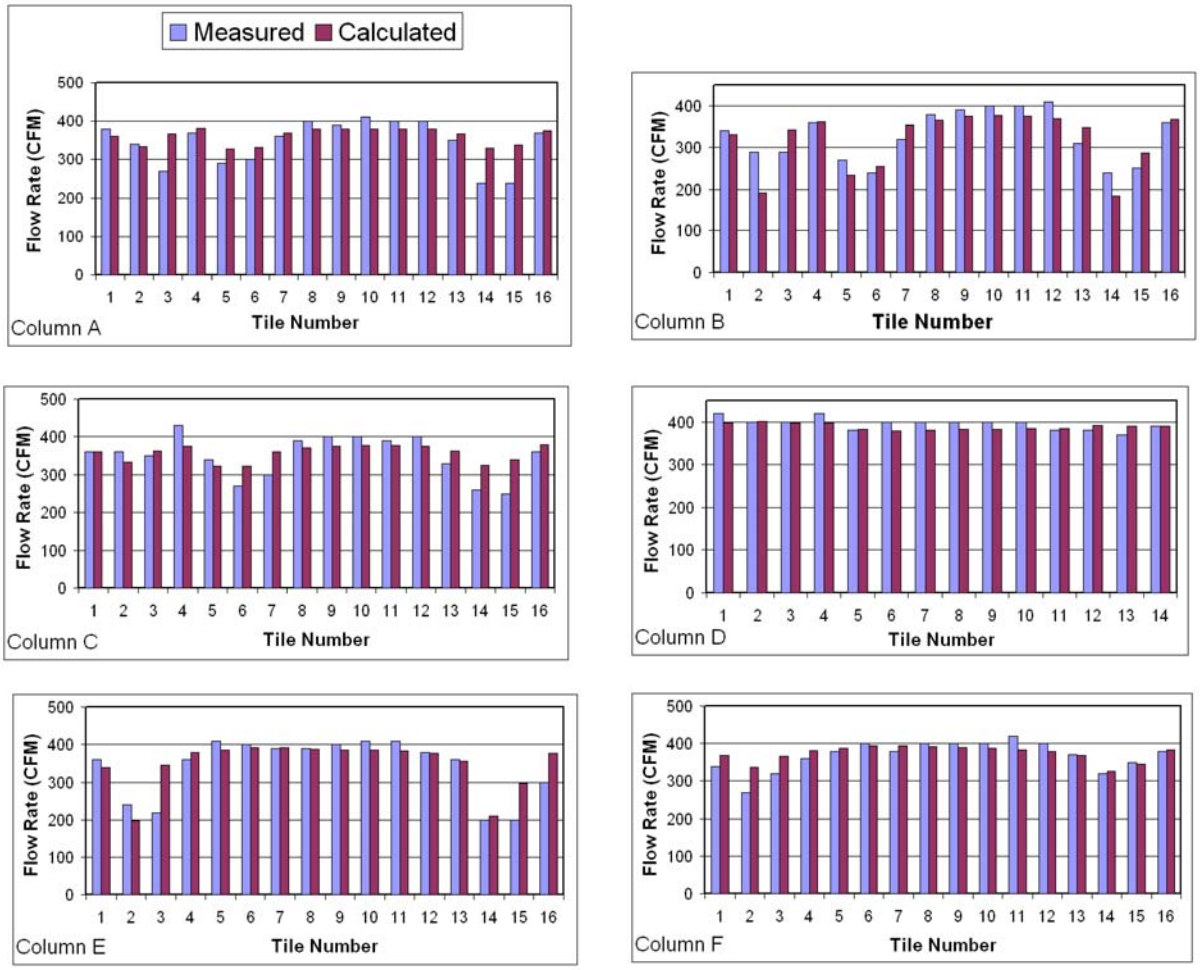

Figure 11
Comparison of measured and calculated flow rates for selected columns of tiles. The columns are identified in Fig. 10.